

Theory of stellar population synthesis with an application to N-body simulations

S. Pasetto¹, C. Chiosi², D. Kawata¹

¹ University College London, Department of Space & Climate Physics, Mullard Space Science Laboratory, Holmbury St. Mary, Dorking Surrey RH5 6NT, United Kingdom

² Department of Physics and Astronomy "Galileo Galilei", University of Padova, Padova, Italy

Accepted for publication in A&A

ABSTRACT

Aims. We present here a new theoretical approach to population synthesis. The aim is to predict colour magnitude diagrams (CMDs) for huge numbers of stars. With this method we generate synthetic CMDs for N-body simulations of galaxies. Sophisticated hydrodynamic N-body models of galaxies require equal quality simulations of the photometric properties of their stellar content. The only prerequisite for the method to work is very little information on the star formation and chemical enrichment histories, i.e. the age and metallicity of all star-particles as a function of time. The method takes into account the gap between the mass of real stars and that of the star-particles in N-body simulations, which best correspond to the mass of star clusters with different age and metallicity, i.e. a manifold of single stellar populations (SSP).

Methods. The theory extends the concept of SSP to include the phase-space (position and velocity) of each star. Furthermore, it accelerates the building up of simulated CMD by using a database of theoretical SSPs that extends to all ages and metallicities of interest. Finally, it uses the concept of distribution functions to build up the CMD. The technique is independent of the mass resolution and the way the N-body simulation has been calculated. This allows us to generate CMDs for simulated stellar systems of any kind: from open clusters to globular clusters, dwarf galaxies, or spiral and elliptical galaxies.

Results. The new theory is applied to an N-body simulation of a disc galaxy to test its performance and highlight its flexibility.

1. Introduction

In the past few decades the unprecedented development of the computational facilities drastically increased the number of NB-based astrophysical simulations. In some areas of astrophysics, this powerful approach represents the only viable laboratory experiment because gravitational interaction on an astrophysical scale is clearly impossible to reproduce in any laboratory.

Since the pioneering works of von Hoerner (1960) and Aarseth (1963), the orbit integration techniques for the NB problem (with N the number of gravitationally interacting bodies) greatly improved (see, e.g., Hockney & Eastwood 1988; Aarseth 2003) both theoretically, with the developments of the tree-codes, particle-mesh (PM), particle-particle-particle mesh (P³M) or see, e.g., Dehnen & Read (2011) for a recent review, and technically, by exploiting the message-passing-interface protocol for the use of massively parallel machines. Although that the N-body simulations were originally conceived as a tool to follow the integration of the orbits, the importance of including energy dissipative processes soon became evident. The treatment of baryonic interactions in N-body simulations is nowadays standardised by popular protocols such as smoothed particle hy-

drodynamics (SPH) or adaptive-mesh-refinement¹ (AMR) implemented in several codes, e.g., Algodoo (e.g., Koreš 2012), DualSPHysics (e.g., Gomez-Gesteira et al. 2012), SPH-flow (e.g., Oger et al. 2006), ENZO (e.g., O'Shea et al. 2004), EvoL (e.g., Merlin et al. 2010), GCD+ (e.g., Kawata & Gibson 2003), GADGET (e.g., Springel et al. 2001), Gasoline (e.g., Wadsley et al. 2004), FLASH ? or RAMSES (e.g., Teyssier 2010; Few et al. 2012), which also includes (in astrophysical context) a sticky-particle approach (Bournaud & Combes 2002; Martig & Bournaud 2010). Thus, even though the recipes for implementing the physics of dissipative phenomena are still controversial, several NB codes are currently able to evolve with time the baryonic component, i.e. gas and stars, in their mutual interaction. Therefore, it is nowadays possible and mandatory to develop the right tools to compare the results of dynamical N-body simulations with observational data for the stellar content of galaxies.

Tantalo et al. (2010) recently developed a technique to derive the integrated spectra, magnitudes and colours of the stellar content of simulated galaxies. These authors focused on the evolution of non-resolved stellar populations and exploited the concept of the spectral energy distribu-

¹ Although AMR codes are not an NB-type code, they often use star-particles to describe the stellar components. Therefore, we here include AMR for our terminology of N-body simulations in this paper.

tion (SED) of an SSP in the context of discrete resolved-mass points of an N-body simulation. There, the integrated monochromatic flux in a given photometric system (set of discrete pass-bands $\Delta\lambda$) of a galactic stellar component at the time t and metallicity Z , $F_\lambda(Z; t)$, is taken to be the convolution of the star formation rate (SFR) $\psi(Z; t)$ (which is assumed to depend only on age and metal content), and the integrated monochromatic flux of constituent SSPs, $\phi_\lambda(Z; t)$, i.e. $F_\lambda(Z; t) = \psi(Z; t) * \phi_\lambda(Z; t)$ ².

In this study we present a new theory of population synthesis that is particularly designed to manage very many stars, and is based on the concept of a distribution function (DF). We focus then on generating the CMDs for the stellar system which are simulated with advanced hydro-dynamical N-body simulation techniques. The subject is particularly timely in view of the modern capabilities of data acquisition of star-by-star photometry in nearby galaxies. This is thanks to modern instrumentation already in place or in progress for the coming years, and also in view of the N-body simulations of model galaxies, in which sampling of either real or fake stars with many millions of objects is possible.

The only prerequisite for the method to work is that minimal information about the history of star formation and chemical enrichment is implemented in and read off the N-body simulations. For each star-particle of the N-body simulation we must know the age at which it was born and the chemical composition (metallicity) of the parental medium. The new formulation of population synthesis takes naturally into account the gap between the mass of the real stars and the mass of the star-particles in N-body simulations if these latter are closer to the mass of a star cluster than the mass of a real star. Therefore the star-content of an N-body simulation is better described as a manifold of star clusters with different age and metallicity, i.e. a manifold of SSP whose photometric properties, primarily the CMD, are well known. Second, CMDs containing an arbitrary number of stars can be easily simulated by defining and making use of the concept of DF of stars in the CMD.

This novel technique is applicable to the stellar content of single open/globular clusters, to our own Galaxy, to that of nearby galaxies within the Local Group, and to all galaxies of the local Universe whose stellar content can be resolved into stars. Moreover, the algorithm can be easily interfaced with other codes, e.g. Galaxia (e.g., Sharma et al. 2011), or the Galaxy Simulators HRD-GST (e.g., Ng et al. 1995, 1996; Ng & Bertelli 1996; Ng et al. 2002a,b; Vallenari et al. 2006), and Besancon model (e.g., Robin et al. 2003), thus extending their performances with the advantages that will become soon clear in what follows.

Setting up the new technique, we focused our attention on a few key requirements that should be met:

1. The algorithm has to be independent of the particular N-body simulation it is applied to. Thus, it is designed to accept the output of a simulation as input, without interfering with the NB integration.

2. The algorithm must not depend on the specific prescriptions used to generate the stellar models that are adopted to describe the composite stellar populations and associated CMDs.
3. The technique needs to handle CMDs populated by several billions of stars, i.e. which are potentially representative of the largest systems of stars known (e.g., giant elliptical galaxies). Indeed, our algorithm should be applicable to every resolved stellar population no matter what the nature of the stellar system under consideration. Therefore CMDs for giant elliptical or spiral galaxies that contain up to 10^{12} stars have to be synthesized with agility.
4. Finally, we require the code to only require little computational resources. The typical CMD of point 3, has to be obtained on a serial machine, i.e. its realization has to avoid more complicated MPI/OpenMP programming protocols.

To achieve those goals, we have developed a method for synthesising CMDs that takes all the above requirements into account. The plan of the paper is as follows: in Section 2 we extend some of the theory concepts of the stellar populations within the framework of the DFs. In Section 3 we particularise the general theory to the case of the N-body simulations. In Section 4 we deal with the simulations of CMDs that contains huge numbers of stars. In Section 5 we present an example of a synthetic CMD realization. In Section 6 we show an example of the technique. Finally we draw some concluding remarks in Section 7 and briefly mention some possible applications of the new method to the synthesis of stellar populations.

2. Theory of Stellar Populations

We extend here the theory of stellar populations to systems (assemblies of stars) with an assigned distribution in the phase-space. This completes the standard theory of stellar populations (e.g., Salaris & Cassisi 2005; Greggio & Renzini 2011) by assigning a position and velocity to each star.

Every real (or realistically simulated) stellar system is a set of stars born at different times and positions, and with different velocities, masses and chemical compositions. We call this assembly of stars *composite-stellar-population* (CSP). The position \mathbf{x} of each star of a CSP is a point in the space \mathbb{X} of coordinates (or space of configurations), and its linear momentum \mathbf{p} is geometrically referred to as a fiber of the cotangent space $T_{\mathbf{x}}^*\mathbb{X}$ of \mathbb{X} at \mathbf{x} (Jose & Saletan 1998). Therefore, the phase-space of a CSP is the cotangent bundle $T^*\mathbb{X} \equiv \bigcup_{\mathbf{x}} T_{\mathbf{x}}^*\mathbb{X}$ of its configuration

space \mathbb{X} . It follows that $T^*\mathbb{X}$ is a $\dim[T^*\mathbb{X}] = 6N$ manifold, with N the total number of stars in the CSP. Each point in it defines the phase-space of our CSP. We indicate this manifold with the symbol Γ , i.e. $\Gamma \equiv T^*\mathbb{X}$ where $\Gamma = (\mathbf{x}, \mathbf{v}) = (x_1, x_2, \dots, x_{3N}, v_1, v_2, \dots, v_{3N})$. Moreover, to completely define the CSP parameters at a generic time t , we need to specify the distribution in the space of the masses, M , and metallicities, Z of all its members. We call this extended phase-space the *existence-space* of the CSP, i.e. $\mathbb{E} \equiv M \times Z \times \Gamma$ of the CSP at the time t and $\mathbb{E} \times \mathbb{R}$ the *extended-existence-space with time t* . In $\mathbb{E} \times \mathbb{R}$, the stars evolve with time, i.e. they continuously move in space, lose mass, enrich in metals, and move in the phase-space. Hence

² Where $f * g$ is the standard convolution operator between the generic functions f and g . In general, we can indeed always write $F_\lambda = L^{-1}[L[\psi]L[\phi_\lambda]]$, with $L[\psi]$ the discrete Laplace transform of the SFR we obtain directly from the N-body simulations and $L[\phi_\lambda]$ the Laplace transform of the monochromatic integrated flux of the a simple stellar population.

we can safely define in \mathbb{E} the distribution function (DF) for the CSPs under the assumption of continuity and differentiability. Let us consider a sample of identical systems whose initial conditions span a certain volume of the space \mathbb{E} . We refer to this sample simply as an *ensemble*, borrowing the name-root from the grand microcanonical ensemble adopted in Statistical Mechanics. The number of systems dN at the time t with mass within dM , metallicity within dZ and phase-space within $d\mathbf{\Gamma} = (d\mathbf{x}, d\mathbf{v})$ is given by

$$dN = N f_{\text{CSP}}(M, Z, \mathbf{\Gamma}; t) dM dZ d\mathbf{\Gamma}, \quad (1)$$

with $f_{\text{CSP}}(M, Z, \mathbf{\Gamma}; t)$ the DF in \mathbb{E} , $f_{\text{CSP}} : \mathbb{R}^+ \times \mathbb{R}^+ \times \mathbb{R}^{6N} \times \mathbb{R} \rightarrow \mathbb{R}^+$ continuous and with partial derivative continuous (where \mathbb{R} is the set of all real numbers, and $\mathbb{R}^+ = \{a | a \in \mathbb{R} \wedge a \geq 0\}$) and the total number of systems in the *ensemble* is fixed by normalising to one the DF in the space \mathbb{E} , i.e.

$$\int f_{\text{CSP}}(M, Z, \mathbf{\Gamma}; t) dM dZ d\mathbf{\Gamma} = 1. \quad (2)$$

We proceed to formally *define* an SSP as follows. At a given time t , we divide \mathbb{E} into a grid in terms of discrete intervals of metallicity dZ and phase-space $d\mathbf{\Gamma}$. Then every infinitesimal unit (i.e. every elementary cell) of this sub-space of \mathbb{E} defines an SSP.

We assume that every CSP originates at time t_0 from an episode of single star formation in a chemically homogeneous medium. The stars of the CSP have the mass spectrum $f_M = f_M(M, t_0) \propto \xi(M, t_0)$ where $\xi(M, t_0)$ is the initial mass function (IMF). Their metallicity distribution is $f_Z = f_Z(t_0) \propto Z_{\text{CSP}}(t_0)$. Finally, their phase-space distribution function is $f_{\mathbf{\Gamma}} = f_{\mathbf{\Gamma}}(\mathbf{\Gamma}; t_0)$. The DF of the CSP can be written as

$$f_{\text{CSP}} = \sum_{i=0}^n f_{\text{SSP}}, \quad (3)$$

where n is the number of SSP, with eventually $n \rightarrow \infty$, and $f_{\text{SSP}} = f_{\text{SSP}}(M, Z_0, \mathbf{\Gamma}_0; t_0)$ is the DF of SSP of which $Z = Z_0$, $\mathbf{\Gamma} = \mathbf{\Gamma}_0$, $t = t_0$ are the metallicity, SSP's phase-space and age at the instant t_0 , respectively.

As time elapses, this stellar population ages. According to their mass, the stars eventually leave the main-sequence (MS) after a time $t_{\text{MS}} = t_{\text{MS}}(M)$ and soon after die (supernovae) or enter a quiescence stage (white dwarfs), injecting metals into the interstellar medium in form of supernova explosions or quiet winds. The interstellar medium becomes richer in metals due both to self-enrichment by the SSP under consideration and the contribution from all other stellar SSPs. At the generic time $t > t_0$, i.e. after an elapsed time $\tau \equiv t - t_0$ otherwise known as the age of the stellar population, the SSP has processed stellar material. As a result of this activity, an age-metallicity relationship $Z_{\text{CSP}} = Z_{\text{CSP}}(t)$ is built up for the CSP.

In addition to this, the number of trajectories in the phase-space entering a volume $d\mathbf{\Gamma}$, will in general be different from the number of those leaving the same volume. Thus $f_{\mathbf{\Gamma}}$ evolves following Liouville's equation of the form

$$\frac{\partial f_{\mathbf{\Gamma}}}{\partial t} = -\iota \mathcal{L} f_{\mathbf{\Gamma}} = - \left(\frac{\partial}{\partial \mathbf{\Gamma}} \cdot \dot{\mathbf{\Gamma}} + \dot{\mathbf{\Gamma}} \cdot \frac{\partial}{\partial \mathbf{\Gamma}} \right) f_{\mathbf{\Gamma}}, \quad (4)$$

which is independent of the nature of the equation of motion (e.g., its correctness in the form of Eq. (4) does *not* require the existence of a Hamiltonian). \mathcal{L} is the Liouvillean

operator, eventually extended to account for a creation function $C(f_{\text{CSP}}; t)$, and ι the imaginary unit. The formal solution of this equation is given by the Taylor expansion series of the time dependence of $f_{\mathbf{\Gamma}}(\mathbf{\Gamma}; t)$ around $f_{\mathbf{\Gamma}}(\mathbf{\Gamma}; t_0)$

$$f_{\mathbf{\Gamma}} = e^{-\iota \mathcal{L} t} f_{\mathbf{\Gamma}}(\mathbf{\Gamma}; t_0) = \sum_{m=0}^{\infty} \frac{(-t)^m}{m!} \frac{\partial^m}{\partial t^m} f_{\mathbf{\Gamma}}(\mathbf{\Gamma}; t_0), \quad (5)$$

and $e^{-\iota \mathcal{L} t} = \sum_{m=0}^{\infty} \frac{(-t)^m}{m!} (\iota \mathcal{L})^m$ defines the infinite series of operators applied on any function on its right side. In this way, the initial SSP has generated a CSP whose distribution in the existence space of the CSP, \mathbb{E} , has a DF $f_{\text{CSP}}(M, Z, \mathbf{\Gamma}; t)$.

Now that we have stated these fundamental concepts, it is easy to proceed with the following formal definitions to recover the usual concepts of the classical synthesis of population theory:

- **Present-day-mass-function:** The integral of the DF over the metallicity Z and phase-space $\mathbf{\Gamma}$ (from Eq. (1))

$$\int N f_{\text{CSP}}(M, Z, \mathbf{\Gamma}; t) dZ d\mathbf{\Gamma} = \hat{\xi}(M; t), \quad (6)$$

yields the “present”-day-mass-function $\hat{\xi}(M; t)$ (PDMF), i.e. the total number of stars per mass interval at the time t . This can be expressed by the approximate relation

$$\hat{\xi}(M; t) = \begin{cases} \xi(M) \frac{t_{\text{MS}}}{t - t_0} & t_{\text{MS}} < \tau \\ \xi(M) & t_{\text{MS}} > \tau, \end{cases} \quad (7)$$

where $\xi(M)$ is IMF of the MS stars. More fine-tuned approaches based on the evolutionary flux, total luminosity and fuel-consumption theorem can be easily worked out upon necessity.

- **Age-metallicity function:** Integrating the DF over the mass M and phase-space $\mathbf{\Gamma}$

$$\int N f_{\text{CSP}}(M, Z, \mathbf{\Gamma}; t) d\mathbf{\Gamma} dM = \chi(Z, t), \quad (8)$$

we obtain the age-metallicity relation, i.e. the number of stars formed per metallicity interval at the time t .

- **The phase-space distribution-function:** Integrating upon the mass M and metallicity Z

$$\int M f_{\text{CSP}}(M, Z, \mathbf{\Gamma}; t) dM dZ = e^{-\iota \mathcal{L} t} f_{\mathbf{\Gamma}}(\mathbf{\Gamma}; t_0), \quad (9)$$

where we made use of Eq. (5), yields the the phase-space DF.

In a natural way, we can extend the approach used in defining Eqs. (6), (8) and (9) by performing the following monodimensional integration:

Metallicity phase-space relationship: We consider the following integration

$$\eta(Z, \mathbf{\Gamma}; t) \equiv \int f_{\text{CSP}}(M, Z, \mathbf{\Gamma}; t) dM \quad (10)$$

to define the metallicity-phase-space relationship. Very often the projection of this function onto the configuration space is used

$$\int \eta(Z, \mathbf{\Gamma}; t) d^{3N} \mathbf{v} = \hat{\eta}(Z, \mathbf{x}; t), \quad (11)$$

where $d^{3N} \mathbf{v}$ is the 3N velocity element of the $\mathbf{\Gamma}$ space. This plays an important role, e.g., in relation to radial metallicity gradients of resolved populations in external galaxies and the vertical metallicity gradients in the Milky Way, i.e. $\hat{\eta}(Z, \mathbf{x}; t) = 0 \forall t$ can implicitly define a function that relates the metallicity Z and the radius of a galaxy R once cylindrical coordinates are in use.

Mass-phase-space relationship: In the same way we define

$$\mu(M, \mathbf{\Gamma}; t) \equiv \int f_{\text{CSP}}(M, Z, \mathbf{\Gamma}; t) dZ, \quad (12)$$

i.e. the mass-phase-space relation. More often its projection onto the configuration space

$$\int \mu(Z, \mathbf{\Gamma}; t) d^{3N} \mathbf{v} = \hat{\mu}(Z, \mathbf{x}; t) \quad (13)$$

is used, which is related, e.g., to the evolution of the globular clusters and the mass-segregation effects, i.e. we can use it to express the higher concentration of massive (or binary stars) through the centre of the cluster with respect to the less massive stars (e.g., Spitzer 1987).

Mass-Metallicity relationship: Finally, we define

$$\varpi(M, Z; t) \equiv \int f_{\text{CSP}}(M, Z, \mathbf{\Gamma}; t) d\mathbf{\Gamma}, \quad (14)$$

i.e. the mass-metallicity relation for a resolved stellar population. This relation is of paramount importance e.g., when the masses of the stars are obtained by parallaxes, transits, and astero-seismology. For nearby galaxies this relation is relevant only in studies of integrated photometry.

3. Stellar populations in N-body simulations

The concepts we have just developed can be straightforwardly applied to N-body simulations of any kind, from those for globular clusters with single or multiple stellar populations (e.g., Milone et al. 2012; Norris 2004), to those for the Milky Way stellar fields observed along any line of sight (e.g., Ng et al. 1995; Vallenari et al. 2006), to the dwarf galaxies of the Local Group (e.g., Grebel 1997; Mateo 1998; Tolstoy et al. 2009), or even external galaxies once they are resolved into individual stars (e.g., Harris & Harris 2002; Rejkuba et al. 2011; Crnojević et al. 2011). Indeed, in the adopted formulation, all the dynamical aspects of the processes governing the formation of the astronomical object under investigation are considered through the most general Liouvillean operator, whose form can be specified case by case. In this context, it is worth recalling that a mutual dependence of star formation, which is responsible for the building up of the stellar population of a stellar system, and the dynamical processes that govern the large scale aggregation of it, is in general supposed to occur in extended many-body interactions (e.g. Pasetto et al. 2011, 2012).

Star-particles in N-body simulations: Before proceeding further, we must suitably link the definition and properties of CSPs to the elemental building blocks of N-body simulations, i.e. the “star-particles”.

We *define* an N-body simulation as a stochastic realization of $f_{\text{CSP}}(M, Z, \mathbf{\Gamma}; \tau)$ in the existence space \mathbb{E} of the CSPs. We focus our attention on the evolution of a single star-particle in an N-body simulation. This particle p is born at the instant $t_{0,p} \equiv t_p$ with metallicity $Z_p = Z_p(t_p)$, at a position in the single particle phase-space γ (a sub-manifold of $T^*\mathbb{X}$) given by $\gamma_p = \gamma_p(t_p)$, with a certain metallicity $Z = Z(t_p)$ (the metal content of the parent gas component at time t_p), and with a mass $M_p = M_p(t_p)$.

The mass of the star-particles and the smaller mass resolution \tilde{M} of the N-body simulations is one of the greatest problems of modern computational N-body simulations and companion mathematical techniques. Apart from a few recent N-body simulations that were specifically tailored for star clusters (e.g., Hut et al. 2003; Zonoozi et al. 2011; Pelupessy & Portegies Zwart 2012), the particle mass of the modern N-body simulations dedicated galaxies and galaxy clusters can vary within a wide range, typically $\log_{10}(\tilde{M}) \simeq 2 \div 8$ (e.g., Saitoh et al. 2009, 2008; Guedes et al. 2011; Okamoto & Frenk 2009). This means that the average mass of the star-particles in the NB simulations is larger than the average mass of the stars in a SSP. Therefore each star-particle is representative (in mass) of many hundreds stars (or more). However, since all stars in a star-particle of a simulation are assumed to be born at the same time with the same metallicity, the stellar content of the star-particle itself is well described by an SSP (see SSP definition in Section 2). Nevertheless, NB simulations cannot easily describe the phase-space distribution of individual stars within a star-particle. In this paper we assume that all stars within each star-particle share the same position in the phase-space. As a consequence of this, the volume of the existence space \mathbb{E} occupied by elemental cells is bounded by the mass resolution, say $d\mathbb{E}_{\text{min}} \equiv dM_p \times dZ \times d\mathbf{\Gamma}$, and it is generally larger than the volume necessary to properly map a CSP, $d\mathbb{E} \equiv d\tilde{M} \times dZ \times d\mathbf{\Gamma}$.

On one hand, if the problem clearly shows that attempts to map the complete IMF are at present out of reach, this indicates on the other hand how a possible solution has to be searched for in the concept of SSP itself.

In an N-body simulation, at the time $t > t_p$ a star-particle is located in $\gamma_p = \gamma_p(t)$, has metallicity $Z_p = Z_p(t)$ and mass $M_p = M_p(t)$. Therefore, mass, metallicity and position in the single-particle phase-space univocally identify the NB-particle all along its evolutionary history from $t_p = t_{0,p}$ to t . At the initial time t_p for each particle p we can associate an SSP to the star-particle in a natural way, provided that some re-scaling of the SSP mass, M_{SSP} , is made in relation to the star-particle mass, M_p . From Eq. (2), the total mass of the SSP can be written as follows:

$$\begin{aligned}
 & \int MN f_{\text{CSP}}(M, Z, \mathbf{\Gamma}; t) \delta(Z - Z_p, \mathbf{\Gamma} - \mathbf{\Gamma}_p, t - t_p) dM dZ d\mathbf{\Gamma} \\
 &= \int MN f_{\text{CSP}}(M, Z_p, \mathbf{\Gamma}_p; t_p) dM \\
 &= \int M \hat{\xi}(M; t_p) dM \\
 &= \int M \xi(M) dM = M_{\text{SSP}}(t_p),
 \end{aligned} \tag{15}$$

where δ is the ordinary multidimensional Dirac function, and in the last row we used Eq. (7) with $t_p = t_{0,p} = 0 < t_{\text{MS}} \forall M$. In other words, the SSP mass written in terms of the DF f_{CSP} or the IMF.

In the same way, we can cast the DF $f_{\text{CSP}}(M, Z, \mathbf{\Gamma}; t)$ of the CSP as a function of the star-particle mass M_p and vice versa. The following identities can be written:

$$\begin{aligned}
 & \int \frac{M_p}{M_{\text{SSP}}} MN f_{\text{CSP}}(M, Z_p, \mathbf{\Gamma}_p; t_p) dM \\
 &\equiv \int MN f_{\text{CSP},p}(M, Z_p, \mathbf{\Gamma}_p; t_p) dM \\
 &= \int MN f_{\text{SSP},p}(M, Z_p, \mathbf{\Gamma}_p; t_p) dM \\
 &= M_p(t_p).
 \end{aligned} \tag{16}$$

While associating the SSP to a generic star-particle born at time t_p with metallicity $Z_p(t_p) = Z_p$ and mass $M_p(t_p) = M_p$ is straightforward, at a generic time $t > t_p$ it is no longer so simple. But if the mass and metallicity of a star-particle do not change with time, the SSP associated to a generic star-particle will simply evolve and age, losing a certain amount of mass in form of gas, changing a fraction of its living stars into remnants, and changing its spectral and photometric properties in a way that is fairly well known from the theory of stellar evolution and population synthesis (e.g., Tosi et al. 1991; Bertelli et al. 1994; Tolstoy & Saha 1996; Aparicio et al. 1997; Harris & Zaritsky 2001; Gallart et al. 2005; Bertelli et al. 2008, 2009).

4. Huge CMDs at no cost

With the formalism we developed on the basis of the CMD of CSP, we now tackle the key question: how can we build CMDs for billions of stars in practice at less computational cost? Because real CPS are the result of the past history of star formation in clusters and fields at the complexity levels of galaxies, how can we easily achieve the same level of information in numerical simulations?

4.1. Associating an SSP to a star-particle

The SSP corresponding to the p^{th} star-particle is obtained by two-dimensional interpolation (in age and metallicity). The number of stars $d\nu_p(L, T_{\text{eff}})$ for the interval of luminosity L and effective temperature T_{eff} , $dLdT_{\text{eff}}$ results from

$$d\nu_p(T_{\text{eff}}, L) = f_{\text{SSP},p} \left[\left[\frac{d(\tau, Z)}{d(T_{\text{eff}}, L)} \right] \right] dT_{\text{eff}} dL, \tag{17}$$

where we referred, by extension of the Jacobean-matrix formalism, with $\left[\left[\frac{d(\tau, Z)}{d(T_{\text{eff}}, L)} \right] \right]$ to the transformation applied on two of the dimensions in which SSP is defined: from age-metallicity space to the effective temperature - luminosity space. Or analogously,

$$d\nu_p(C, m) = f_{\text{SSP},p} \left[\left[\frac{d(\tau, Z)}{d(T_{\text{eff}}, L)} \right] \right] \left[\left[\frac{d(T_{\text{eff}}, L)}{d(C, m)} \right] \right] dC dm \tag{18}$$

for the same transformation to the space of the colour C and magnitude m . In general there is no analytic formulation for the two matrixes $\left[\left[\frac{d(\tau, Z)}{d(T_{\text{eff}}, L)} \right] \right]$ and $\left[\left[\frac{d(T_{\text{eff}}, L)}{d(C, m)} \right] \right]$. They are derived numerically from the tabulations of bolometric corrections, and colours of, e.g., the Johnson-Cousin-Glass system.

The key idea of Eq. (17) or (18) is to describe a CMD as a matrix, i.e. a projected DF, whose elements are the relative frequency (or percentage) of stars of different colour and magnitude in some photometric system, per elemental area of the CMD. For a given photometric system with passbands $\Delta\lambda_\alpha$ (for instance α stands for U, B, V, ...) for which magnitudes m_α and colours $C_{\alpha\beta} \equiv m_\alpha - m_\beta$ can be computed (magnitudes and colours can be either absolute and intrinsic or apparent and reddened³), Eq. (18) represents a 2D grid of elemental square cells $d\nu_p(C_{\alpha\beta}^c, m_\alpha^c)$, identified by the coordinates of their centres m_α^c and $(m_\alpha - m_\beta)^c$. The path drawn in the CMD by a single SSP of assigned age and chemical composition, see Section 2 and Eq. (18), will occupy a number of cells from the main sequence to the last observable stage. Each cell is populated by a certain number of stars according to the underlying luminosity function of the SSP, which in turn is related to the evolutionary rate and IMF (see Eq. (6) and (7)). If many SSPs are present, as in the case of a composite CSP, each cell contains a total number of stars given by the sum of all contributions by different SSPs passing through this cell. Using Eqs. (3) together with (18), we obtain

$$\nu_p(C_{\alpha\beta}, m_\alpha) = \sum_p d\nu_p(C_{\alpha\beta}, m_\alpha) \tag{19}$$

Therefore, a relative percentage of stars is associated to each cell (matrix element) with respect to the total. The number of stars per cell can be easily normalised according to the problem under investigation. The observational CMDs that contain an arbitrary number of stars, from a few thousands to billions, is reduced to a matrix of number frequencies (relative percentages, Eq. (18)). The prescription can be easily extended to include any history of star formation of any intensity, ψ , as well as kinematical effects ($f_{\mathbf{\Gamma}}$ as in Eq. (5)).

Finally we are left to specify the initial distribution of mass (IMF) and the adopted database of stellar models:

- **The initial mass function:** To calculate an SSP, we need an IMF. The most popular IMF is given by

$$\xi(M) = \xi_0 \sum_{i=1}^k M^{-x_i} \Delta_i \tag{20}$$

³ The same considerations also apply to bolometric luminosities and effective temperatures.

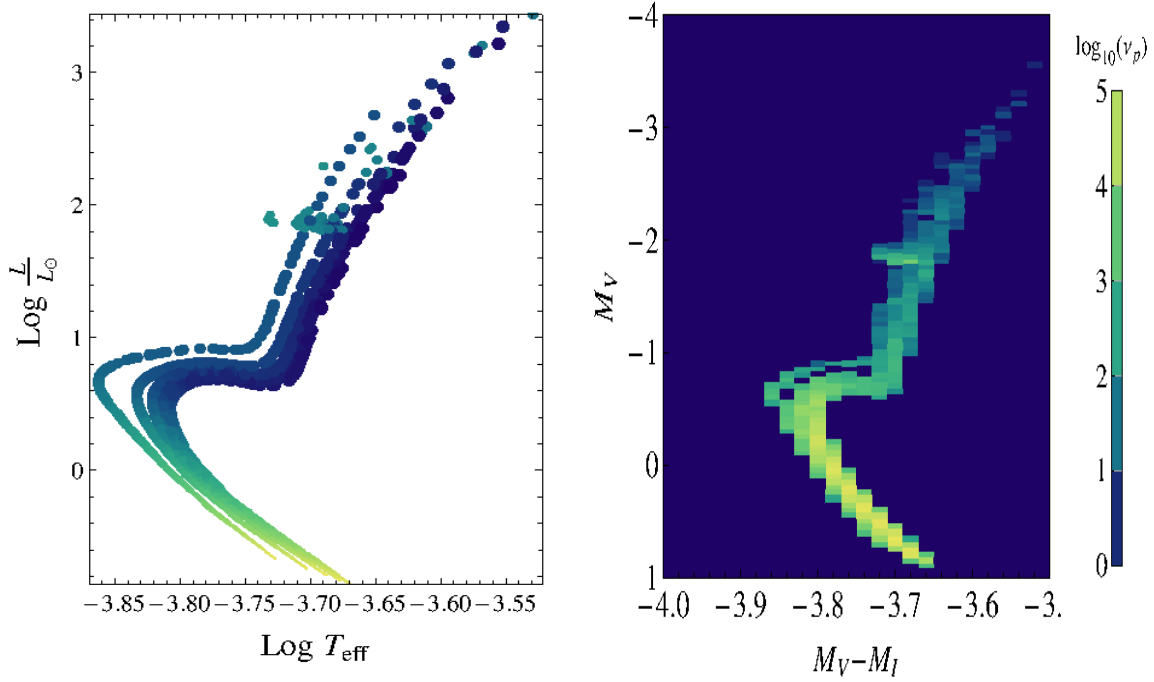


Fig. 1. Left panel: The HRD of SSPs with assigned age and metallicity. The size of the circles indicates the current star mass along the isochrones and/or SSP. The stellar models in use are taken from the library of Bertelli et al. (2008) and Bertelli et al. (2009). The colour code refers to the size of the dots: the smaller is the dot, the more yellow it is and the smaller the mass of the plotted stars. The bigger the dot, the bluer its colour and the bigger the mass of the stars. The mass considered in the models of this example ranges from 0.15 to 20 M_{\odot} . Right panel: The same SSPs displayed in the left panel but in the observational CMD M_V vs $M_V - M_I$. The CMD is subdivided to a discrete grid of elemental cells, in each of which a certain number of stars fall. The stars in each cell may belong to different SSPs. The size of the cell is large clearly show evidence the “out-of-focus” effect intrinsic to this tessellation technique. Colour-code spans account for the number of stars in the cells from 0 (the bluer colour) to 10^5 (the light yellow colour).

with

$$\Delta_i = \begin{cases} 1 & M \in \Delta M_i \\ 0 & M \notin \Delta M_i \end{cases} \quad (21)$$

with ξ_0 normalisation factor of the IMF, $\Delta M_i = \{M_i | M_i \in [M_{\text{low},i}, M_{\text{up},i}]\}$, with $M_{\text{low},i}$ ($M_{\text{up},i}$) lower (upper) limit for the i^{th} -mass interval and $\Delta M_i \cap \Delta M_j = \emptyset$ for $i \neq j$. The case $k = 1$ in Eq. (20) is often referred to as Salpeter’s IMF with power-law slope $x_i = 2.35 \forall i$, the case $k = 3$ is referred as Kroupa’s IMF with its specific slope and intervals (see e.g., Kroupa 2001) or in general any IMF function can be approximated by a sum as in Eq. (20) for a suitable choice of k . Therefore, in the general case, the total number of stars plotted in an SSP is

$$\begin{aligned} N_{\text{SSP}} &= \int_{M_{\text{low}}}^{M_{\text{up}}} \xi_0 \sum_{i=1}^k \Delta_i M^{-x_i} dM \\ &= \xi_0 \sum_{i=1}^k \Delta_i \int_{M_{\text{low}}}^{M_{\text{up}}} M^{-x_i} dM \\ &= \xi_0 \sum_{i=1}^k \frac{\Delta_i}{x_i - 1} \frac{M_{\text{up}}^{x_i - 1} - M_{\text{low}}^{x_i - 1}}{(M_{\text{low}} M_{\text{up}})^{x_i - 1}} \quad x_i \neq 1 \end{aligned} \quad (22)$$

or $N_{\text{SSP}} = \xi_0 \sum_{i=1}^k \Delta_i \log\left(\frac{M_{\text{up}}}{M_{\text{low}}}\right)$ for $x_i = 1$. If we choose to sample all star-phases of higher luminosity (e.g.,

asymptotic giant branch (AGB) and planetary nebula (PNs)) with $N_{\text{SSP}} \cong 10^5$ stars it becomes immediately evident how the graphical realization of a CMD for an N-body simulation encounters serious problems once the number of star-particles involved, N , is high, say $N_{\text{SSP}} \times N \cong O(10^{11 \div 13})$ for $N \sim 10^{6 \div 8}$.

- The database of SSPs: We briefly report here on the database of SSPs that was calculated for the purposes of this study. The stellar models used are those by Bertelli et al. (2008, 2009), which cover a wide grid of helium Y , metallicity Z , and enrichment ratio $\Delta Y/\Delta Z$. The associated isochrones include the effect of mass loss by stellar wind and the thermally pulsing AGB phase according to the models calculated by Marigo & Girardi (2007). The code used is the last version of YZVAR developed over the years by the Padova group used in many studies (for instance Chiosi & Greggio 1981; Chiosi et al. 1986b,a, 1989; Bertelli et al. 1995; Ng et al. 1995; Aparicio et al. 1996; Bertelli & Nasi 2001; Bertelli et al. 2003) and was recently extended to obtain isochrones and SSPs in a large region of the $Z - Y$ plane. The details on the interpolation scheme at a given $\Delta Y/\Delta Z$ are given in Bertelli et al. (2008, 2009).

The present isochrones and SSPs are in the Johnson-Cousins-Glass system as defined by Bessell (1990) and Bessell & Brett (1988). The formalism adopted to derive

the bolometric corrections is described in Girardi et al. (2002), while the definition and values of the zero-points are described in Marigo & Girardi (2007) and Girardi et al. (2007) and will not be repeated here.

Suffice it to recall that the bolometric corrections stand on an updated and extended library of stellar spectral fluxes. The core of the library now consists of the ODFNEW ATLAS9 spectral fluxes from Castelli & Kurucz (2003), for $T_{\text{eff}} \in [3500, 50000]$ K, $\log_{10}g \in [-2, 5]$ (with g the surface gravity), and scaled solar metallicities $[M/H] \in [-2.5, +0.5]$. This library is extended at the intervals of high T_{eff} with pure black-body spectra. For lower T_{eff} , the library is completed with the spectral fluxes for M, L and T dwarfs from Allard et al. (2000), M giants from Fluks et al. (1994), and finally the C star spectra from Loidl et al. (2001). Details about the implementation of this library, and in particular about the C star spectra, are provided in Marigo & Girardi (2007). It is also worth mentioning that in the isochrones we applied the bolometric corrections derived from this library without making any correction for the enhanced He content which has been proved by Girardi et al. (2007) to be low in most common cases.

The database of SSP covers the space of existence \mathbb{E} of a generic CPS. The number of ages N_τ of the SSPs are sampled according to a law of the type $\tau = i \times 10^j$ for $i = 1, \dots, 9$ and $j = 7, \dots, 9$, and for N_Z metallicities are $Z = \{0.0001, 0.0004, 0.0040, 0.0080, 0.0200, 0.0300, 0.0400\}$. The helium content associated to each choice of metallicity is according to the enrichment law $\Delta Y \Delta Z = 2.5$. Each SSP was calculated allowing a small age range around the current value of age given by $\Delta\tau = 0.002 \times 10^j$ with $j = 7, \dots, 9$. In total, the data base contains $N_\tau \times N_Z \cong 150$ SSP. This grid is fully sufficient to illustrate the method. For future practical application of it, finer grids of SSPs can be calculated and made available. Having done this, the normalization constant ξ_0 of the SSPs remains defined. Finally, for each SSP we computed the “projected” DF, i.e. the number of stars per elemental cell of the CMD, using the value of ξ_0 .

Note that the method for generating the cumulative DFs of Eq. (19) from SSPs does not depend on the particular choice for the data base of stellar tracks, isochrones, or photometric system. Other libraries of stellar models and isochrones can be used to generate the database of SSP, the building blocks of our method.

From the procedure outlined above, it is easy to understand how the use of the stellar DF is able to accelerate the construction of the CMD of a CSP. The reason is as follows: Instead of calculating an SSP made by N_{SSP} stars for every star particle of the N-body simulation (i.e., for a total of N star particles) and counting the stars inside a given bin of magnitude and colour $\delta C \delta m$, i.e. summing over $N \times N_{\text{SSP}} \cong O(10^{11 \div 13})$ stars, with the above procedure, we need to calculate only $N_\tau \times N_Z \times N_{\text{SSP}} \cong O(10^7)$ stars. However, the number frequencies per cell of the CMD of our reference SSPs are calculated once for all, whereas their combinations can be freely changed according to the underlying star formation history of the N-body simulation to investigate and the number of calculation required in this method is then just $O(N) \ll 10^{11 \div 13}$.

The left panel of Fig.1 shows a few SSPs for the solar metallicity $Z = 0.02$ and helium content $Y = 0.28$ in the theoretical Hertzsprung-Russell diagram (HRD). The size of the dots is proportional to the stellar mass running along the SSPs. The same SSPs are translated into the M_V vs $M_V - M_I$ plane displayed in the right panel of Fig. 1 in which the cell tessellation is evident. The “out-of-focus” effect is due to grouping the stars of different SSPs into the same cell. No photometric errors are applied.

4.2. Simulation of photometric errors and completeness

We finally mention that real data on the magnitudes (and colours) of the stars are affected by photometric errors, whose amplitude in general increases at decreasing luminosities (increasing magnitude). The photometric errors come together with the data themselves provided they are suitably reduced and calibrated. Photometric errors can be easily simulated in our theoretical CMDs. Suppose we know the errors affecting our magnitudes in the two pass-bands used to build the CMD, and that these are a function of the magnitude itself. Let us indicate the errors by $\delta m_\alpha(m)$, and $\delta m_\beta(m)$, with α and β the two pass-bands. When plotting each point of the SSPs on the observational CMDs, the magnitudes are changed by the quantity representing the errors, e.g.:

$$\begin{aligned} m'_\alpha(m) &= m_\alpha(m) - \left(\frac{1}{2} - r\right) \delta m_\alpha(m) \\ m'_\beta(m) &= m_\beta(m) - \left(\frac{1}{2} - s\right) \delta m_\beta(m), \end{aligned} \quad (23)$$

where r and s are two randomly drawn numbers (e.g., from uniform or Gaussian distribution) comprised between 0 and 1. The star frequencies per elemental cell of the CMD are calculated after applying the correction for photometric errors to the reference SSPs.

To compare the real observational data with the theoretical model we have to know the completeness of the former as a function of the magnitudes and pass-band (Stetson & Harris 1988; Aparicio & Gallart 1995). This is a long known problem that does not require any particular discussion in the context of this paper, and tabulations of the completeness factors must be supplied in advance together with the correction for photometric errors. We mention here is that correcting for completeness will alter the DF of stars in the cells of the observational CMD we aim to analyse (e.g., Crnojević et al. 2011). These completeness factors must be supplied by the user of our method in connection with the specified problem.

5. Generating a CMD with tessellation

To explain the concept of CMD tessellation, we simulated a CMD using the CSP of NB-TSPH simulation (to be described in more detail below). The analysed field contains 8.8×10^4 star-particles of the same mass and known age and metallicity (to each of which an SSP can be associated with the same mass, age and metallicity, see Section 3). For the purpose of this example we show only the absolute luminosity and magnitude, i.e. no distance dependence. The results of applying Eq. (19) are shown in Fig. 2. The left panel displays the frequency distribution of CSP in the $(M_V - M_I)$

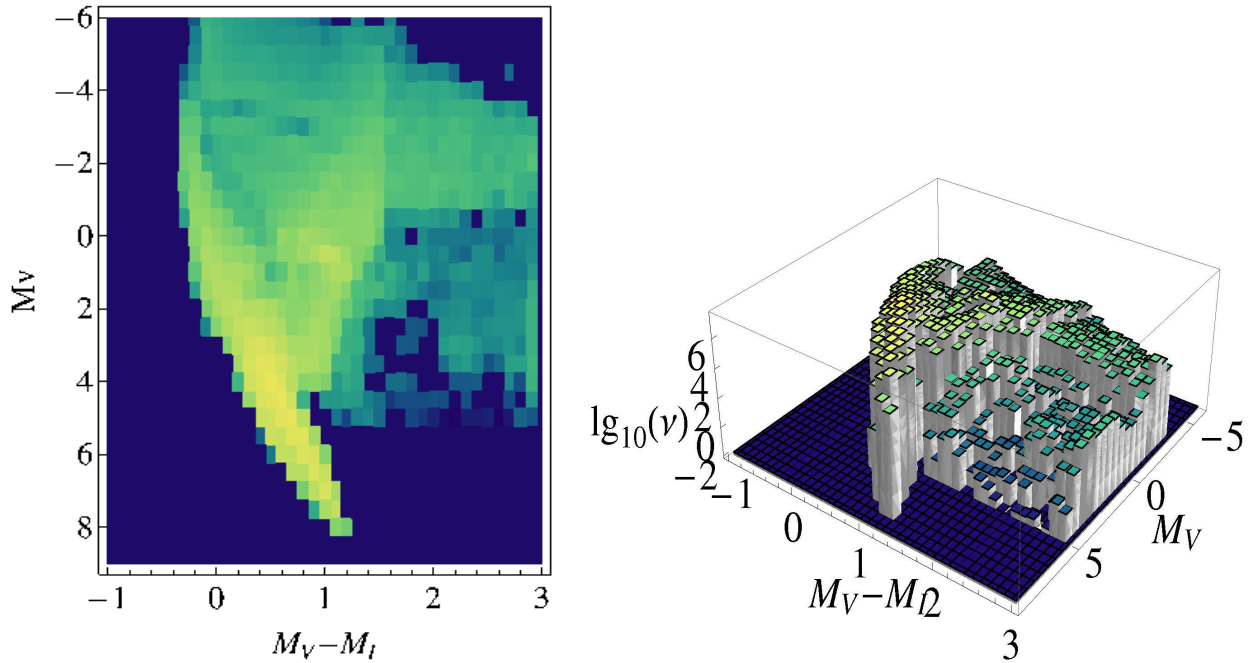


Fig. 2. Left panel: The CSP for an N-body simulation of a disc galaxy. Colour code refers to the frequency of star per bin shown in the companion right panel. Right panel: The histogram of DF for the CSP shown in the left panel. In this figure, one immediately captures the concept of DF described in the text. The characteristic peaks corresponding to MS and RGB stars are shown in yellow. The CMDs have the coordinates of the absolute magnitudes M_V and the colours $M_V - M_I$.

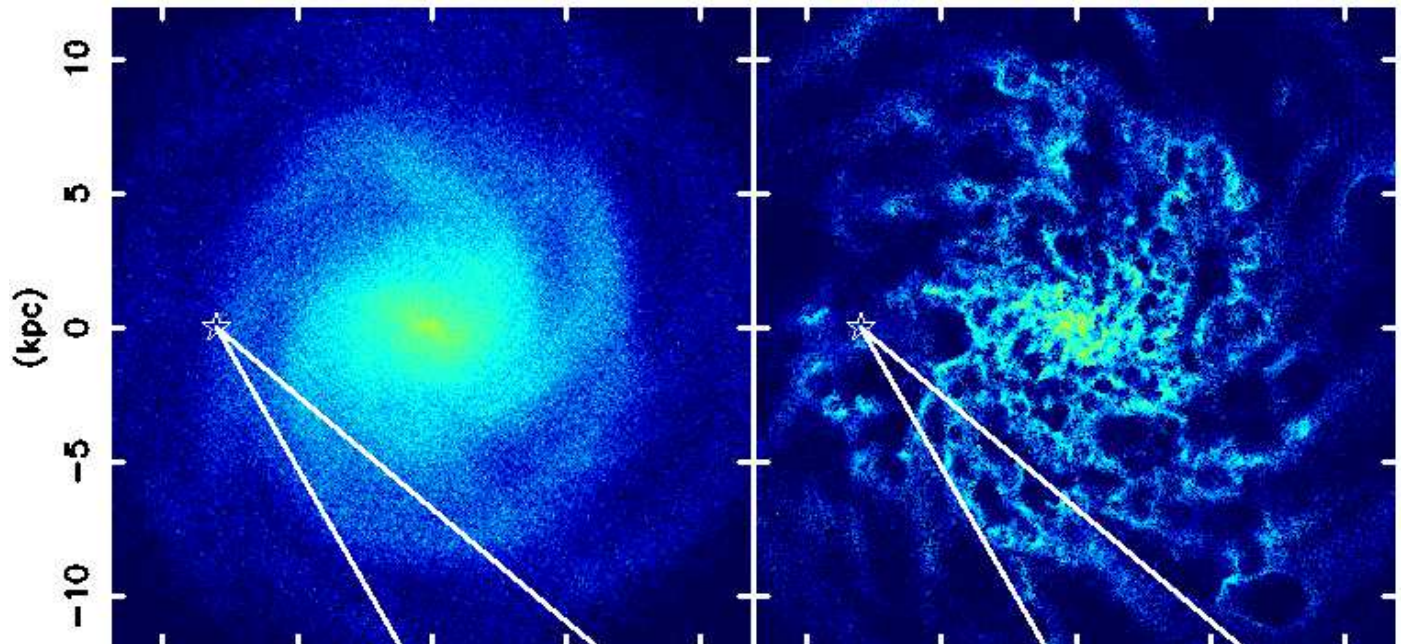


Fig. 3. Snapshot of the simulated disc galaxy whose face-on views of the stellar and gas discs are shown in the left and right panels, respectively. Our assumed location of the Sun is highlighted by a star symbol. The white lines indicate the selected region for constructing the CMD shown in Fig. 5. Colour code ranges from blue (the lowest density) to red (the highest density).

vs M_V CMD, while the right panel shows the histogram. The regions occupied by stars in the main sequence are clearly evident: Long-lived phases display a higher number of stars, on the other hand, red giant, red clump, and asymptotic giant phases are seen in low effective temperatures (red colours) and shows lower frequency due to their short lifetime. These features are similar to a typical observed CMD of the stellar populations in nearby galaxies,

e.g. the Magellanic Clouds, M31 and others, where for all stars in a given galaxy the distance is nearly constant.

6. Application to N-body simulations

To demonstrate the method, we applied it to an N-body simulation. The simulation was carried out with an updated version of our original NB-SPH code, GCD+ (Kawata &

Gibson 2003; Rahimi & Kawata 2012). We initially set up an isolated Milky Way-sized disc galaxy that consists of gas and stellar discs with no bulge component in a static dark matter halo potential, following Rahimi & Kawata (2012). Note that this simulation was used for demonstration purpose, and was not meant to reproduce the Milky Way. We used the standard Navarro-Frenk-White dark matter halo profile (Navarro et al. 1997) with the total mass of $M_{\text{tot}} = 1.5 \times 10^{12} M_{\odot}$ and the concentration parameter of $c = 12$. The mass, scale length and scale high of the stellar disc were assumed to be $M_{\text{d,s}} = 4.0 \times 10^{10} M_{\odot}$, $R_{\text{d,s}} = 2.5$ kpc and $z_{\text{d,s}} = 350$ pc. The mass and scale length of the gas disc was $M_{\text{d,g}} = 1.0 \times 10^{10} M_{\odot}$, $R_{\text{d,g}} = 4.0$ kpc. We initially set 400,000 particles to the gas disc and 1,600,000 particles to the stellar disc. Therefore, our baryon particle mass was $M_{\text{p}} = 2.5 \times 10^4 M_{\odot}$. We applied the threshold density of $n_{\text{H}} = 1.0 \text{ cm}^{-3}$ for star formation. Rahimi & Kawata (2012) demonstrated that the star formation in a disc is quite sensitive to the parameters of star formation efficiency, C_* , energy for supernova, E_{SN} , and stellar wind feedback energy, E_{SW} . We here applied $C_* = 0.1$, $E_{\text{SN}} = 10^{51}$ erg and $E_{\text{SW}} = 10^{37}$ erg s^{-1} . Fig. 3 shows a snapshot of the simulation. Strong feedback creates many bubbles in the gas disc.

The simulated galaxy shows a small bar and several spiral arms. We set the Sun at $(x, y) = (-8, 0)$ kpc (star symbol in Fig. 3), and selected star-particles in the region of the simulated galaxy “equivalent longitude” $300 < l < 320$ and “latitude” $-10 < b < 10$ (with implicit reference to the Milky Way galaxy coordinates system l, b), which is enclosed by white lines in Figs. 3 and 4. For each star-particle we measured the distance and extinction from the simulation. To measure the extinction, first the column density for each star-particle was calculated by summing up the line of sight column density of all gas particles between the star-particle and the position of the Sun, using the SPH weighting scheme (Kawata & Rauch 2007). We then converted the column density to the extinction, using $N_{\text{H}} = 1.9 \times 10^{21} \text{ cm}^{-2} \times A_V(\text{magnitude})$.

The simulation of the CMD for the selected star-particles is shown in Fig. 2 where with a magnitude cut for true stars at above $V > 20$ mag about 8.8×10^4 star-particles within the galaxy coordinates defined above are retained. We recall that Fig. 2 shows absolute magnitude and luminosity, which are independent of the distance. To build the observational CMD we need to take into account distance and extinction for each star-particle, which are measured for each particle as described above. The resulting “observational” CMD is a shown in Fig. 5. With the IMF we assumed that the resulting CMD is representative of about 1.08×10^{10} true stars. The difference in distance and extinction for each star-particle leads to a more smoothly distributed CMD. As a result, the groups of main sequence stars and red giant stars are hardly recognizable in Fig. 5. This is often observed in the photometric data of Galactic stars.

7. Concluding remarks

We first extended the theory of the stellar populations to include the phase-space description. We described the concepts of composite stellar population, simple stellar population, star formation rate, initial mass function, etc. using the language of Statistical Mechanics. Now it is fair

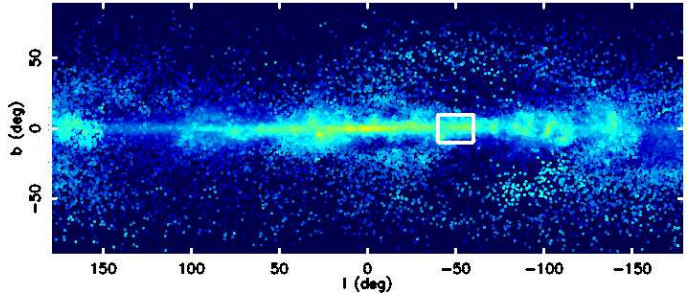


Fig. 4. Gas distribution in a Galactic coordinate of the simulated galaxy shown in Fig. 3. The region enclosed by the white lines are the selected region for constructing the CMD shown in Fig. 5. The colour coding is by density, so that bluer and more yellow points represent higher and lower density particles respectively.

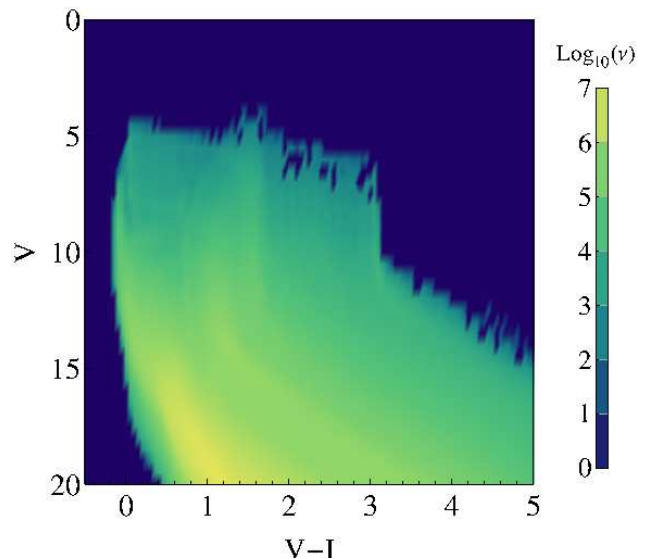


Fig. 5. Observational CMD in apparent magnitudes and colours. The colour-coding is by density, so that bluer and more yellow points represent higher and lower density particles, respectively.

to ask what we have gained from this rather formal approach. These techniques have proven to be extremely powerful in other branches of physics e.g., for the study of relaxation phenomena, electrical conduction, irreversible processes (see e.g., Landau & Lifshitz 2000) or in general for the development of the thermodynamics of non-equilibrium system (see e.g., de Groot & Mazur 1961) while have been more limited in the treatment of long-range forces e.g., the statistical mechanics of gravitational systems (see, e.g., Lynden-Bell & Wood 1968; Katz 2003), therefore it is important to understand to what extent they can be applied to the stellar populations. The mutual benefit between Statistical Mechanics and stellar populations theory consists of the temporal evolution of the existence space we introduced, the projection of which onto the CMD is governed by the fuel consumption theorem that drives the relative number of stars in different evolutionary stages, hence cells of the CMD. Moreover, studying the coupling between dynamics and theory of the stellar populations imprinted in the existence space, may reveal unexplored connections.

The second achievement of this paper is indeed the application of this theory to develop a method for handling the synthetic CMDs that one would generate from N-body simulations, which are to be compared with the CMDs of real galaxies when they are resolvable into stars. The method based on the concept of star frequencies per elemental cell of the CMD can easily simulate observational CMDs that contain huge numbers of stars. This study extends and completes other similar studies in literature that dealt with synthetic CMDs such as those presented by in Carraro et al. (2001); Pasetto et al. (2012). This technique aims to interface N-body simulations to photometric observations and is developed with the perspective of the ever improving capabilities of the N-body simulations in the future. Finally, thanks to its agility, the CMD tessellation method can be suitably interfaced with galaxy models based on star counts (see for instance Vallenari et al. 2006) and other hybrid techniques based on the different approaches already present in literature such as the Galaxia model (see e.g., Sharma et al. 2011) or the Besancon model (see e.g. Robin et al. 2003) and it represents a natural extension of previous work (e.g. Tantalo et al. 2010).

The tessellation code for generating the CMD for N-body simulations is available upon request from the authors.

Acknowledgements. SP acknowledges D. Crnojević and J. Hunt for careful reading of an early version of this manuscript. The authors thank the anonymous referee for the constructive report.

References

- Aarseth, S. J. 1963, MNRAS, 126, 223
Aarseth, S. J. 2003, Gravitational N-Body Simulations, ed. Aarseth, S. J.
Allard, F., Hauschildt, P. H., Alexander, D. R., Ferguson, J. W., & Tamanai, A. 2000, in Astronomical Society of the Pacific Conference Series, Vol. 212, From Giant Planets to Cool Stars, ed. C. A. Griffith & M. S. Marley, 127
Aparicio, A. & Gallart, C. 1995, AJ, 110, 2105
Aparicio, A., Gallart, C., & Bertelli, G. 1997, AJ, 114, 680
Aparicio, A., Gallart, C., Chiosi, C., & Bertelli, G. 1996, ApJ, 469, L97
Bertelli, G., Bressan, A., Chiosi, C., Fagotto, F., & Nasi, E. 1994, A&AS, 106, 275
Bertelli, G., Bressan, A., Chiosi, C., Ng, Y. K., & Ortolani, S. 1995, A&A, 301, 381
Bertelli, G., Girardi, L., Marigo, P., & Nasi, E. 2008, A&A, 484, 815
Bertelli, G. & Nasi, E. 2001, AJ, 121, 1013
Bertelli, G., Nasi, E., Girardi, L., et al. 2003, AJ, 125, 770
Bertelli, G., Nasi, E., Girardi, L., & Marigo, P. 2009, A&A, 508, 355
Bessell, M. S. 1990, PASP, 102, 1181
Bessell, M. S. & Brett, J. M. 1988, PASP, 100, 1134
Bournaud, F. & Combes, F. 2002, A&A, 392, 83
Castelli, F. & Kurucz, R. L. 2003, in IAU Symposium, Vol. 210, Modelling of Stellar Atmospheres, ed. N. Piskunov, W. W. Weiss, & D. F. Gray, 20P
Chiosi, C., Bertelli, G., & Bressan, A. 1986a, Memorie della Societa Astronomica Italiana, 57, 507
Chiosi, C., Bertelli, G., Bressan, A., Nasi, E., & Pigatto, L. 1986b, in Star-forming Dwarf Galaxies and Related Objects, 449–463
Chiosi, C., Bertelli, G., Meylan, G., & Ortolani, S. 1989, A&A, 219, 167
Chiosi, C. & Greggio, I. 1981, A&A, 98, 336
Crnojević, D., Rejkuba, M., Grebel, E. K., da Costa, G., & Jerjen, H. 2011, A&A, 530, A58
de Groot, S. & Mazur, P. 1961, Non-equilibrium thermodynamics
Dehnen, W. & Read, J. I. 2011, European Physical Journal Plus, 126, 55
Few, C. G., Courty, S., Gibson, B. K., et al. 2012, ArXiv e-prints
Fluks, M. A., Plez, B., The, P. S., et al. 1994, A&AS, 105, 311
Gallart, C., Zoccali, M., & Aparicio, A. 2005, ARA&A, 43, 387
Girardi, L., Bertelli, G., Bressan, A., et al. 2002, A&A, 391, 195
Girardi, L., Castellì, F., Bertelli, G., & Nasi, E. 2007, A&A, 468, 657
Gomez-Gesteira, M., Rogers, B., Crespo, A., et al. 2012, Computers & Geosciences
Grebel, E. K. 1997, in Reviews in Modern Astronomy, Vol. 10, Reviews in Modern Astronomy, ed. R. E. Schielicke, 29–60
Greggio, L. & Renzini, A. 2011, Stellar Populations. A User Guide from Low to High Redshift, ed. Greggio, L. & Renzini, A.
Guedes, J., Callegari, S., Madau, P., & Mayer, L. 2011, ApJ, 742, 76
Harris, J. & Zaritsky, D. 2001, ApJS, 136, 25
Harris, W. E. & Harris, G. L. H. 2002, AJ, 123, 3108
Hockney, R. W. & Eastwood, J. W. 1988, Computer simulation using particles
Hut, P., Shara, M. M., Aarseth, S. J., et al. 2003, New A, 8, 337
Jose, J. V. & Saletan, E. J. 1998, Classical dynamics : a contemporary approach, ed. Jose, J. V. & Saletan, E. J.
Katz, J. 2003, Found.Phys
Kawata, D. & Gibson, B. K. 2003, MNRAS, 340, 908
Kawata, D. & Rauch, M. 2007, ApJ, 663, 38
Koreš, J. 2012, The Physics Teacher, 50, 278
Kroupa, P. 2001, MNRAS, 322, 231
Landau, L. & Lifshitz, E. 2000, Statistical Physics
Loidl, R., Lançon, A., & Jørgensen, U. G. 2001, A&A, 371, 1065
Lynden-Bell, D. & Wood, R. 1968, MNRAS, 138, 495
Marigo, P. & Girardi, L. 2007, A&A, 469, 239
Martig, M. & Bournaud, F. 2010, ApJ, 714, L275
Mateo, M. L. 1998, ARA&A, 36, 435
Merlin, E., Buonomo, U., Grassi, T., Piovan, L., & Chiosi, C. 2010, A&A, 513, A36
Milone, A. P., Piotto, G., Bedin, L. R., et al. 2012, ApJ, 744, 58
Navarro, J. F., Frenk, C. S., & White, S. D. M. 1997, ApJ, 490, 493
Ng, Y. K. & Bertelli, G. 1996, A&A, 315, 116
Ng, Y. K., Bertelli, G., Bressan, A., Chiosi, C., & Lub, J. 1995, A&A, 295, 655
Ng, Y. K., Bertelli, G., Chiosi, C., & Bressan, A. 1996, A&A, 310, 771
Ng, Y. K., Brogt, E., Chiosi, C., & Bertelli, G. 2002a, A&A, 392, 1129
Ng, Y. K., Brogt, E., Chiosi, C., & Bertelli, G. 2002b, A&A, 392, 1129
Norris, J. E. 2004, ApJ, 612, L25
Oger, G., Doring, M., Alessandrini, B., & Ferrant, P. 2006, Journal of Computational Physics, 213, 803
Okamoto, T. & Frenk, C. S. 2009, MNRAS, 399, L174
O’Shea, B. W., Bryan, G., Bordner, J., et al. 2004, ArXiv Astrophysics e-prints
Pasetto, S., Bertelli, G., Grebel, E. K., Chiosi, C., & Fujita, Y. 2012, A&A, 542, A17
Pasetto, S., Grebel, E. K., Berczik, P., Chiosi, C., & Spurzem, R. 2011, A&A, 525, A99
Pelupessy, F. I. & Portegies Zwart, S. 2012, MNRAS, 420, 1503
Rahimi, A. & Kawata, D. 2012, MNRAS, 2756
Rejkuba, M., Harris, W. E., Greggio, L., & Harris, G. L. H. 2011, A&A, 526, A123
Robin, A. C., Reylé, C., Derrière, S., & Picaud, S. 2003, A&A, 409, 523
Saitoh, T. R., Daisaka, H., Kokubo, E., et al. 2008, PASJ, 60, 667
Saitoh, T. R., Daisaka, H., Kokubo, E., et al. 2009, PASJ, 61, 481
Salaris, M. & Cassisi, S. 2005, Evolution of Stars and Stellar Populations, ed. Salaris, M. & Cassisi, S.
Sharma, S., Bland-Hawthorn, J., Johnston, K. V., & Binney, J. 2011, ApJ, 730, 3
Spitzer, L. 1987, Dynamical evolution of globular clusters
Springel, V., Yoshida, N., & White, S. D. M. 2001, New A, 6, 79
Stetson, P. B. & Harris, W. E. 1988, AJ, 96, 909
Tantalo, R., Chinellato, S., Merlin, E., Piovan, L., & Chiosi, C. 2010, A&A, 518, A43
Teyssier, R. 2010, in Astrophysics Source Code Library, record ascl:1011.007, 11007
Tolstoy, E., Hill, V., & Tosi, M. 2009, ARA&A, 47, 371
Tolstoy, E. & Saha, A. 1996, ApJ, 462, 672
Tosi, M., Greggio, L., Marconi, G., & Focardi, P. 1991, AJ, 102, 951
Vallenari, A., Pasetto, S., Bertelli, G., et al. 2006, A&A, 451, 125
von Hoerner, S. 1960, ZAp, 50, 184
Wadsley, J., Stadel, J., & Quinn, T. 2004, New Astronomy, 9, 137
Zonoozi, A. H., Küpper, A. H. W., Baumgardt, H., et al. 2011, MNRAS, 411, 1989